Development 129, 5839-5846

doi:10.1242/dev.00173



DEVELOPMENT AND DISEASE

# A defect in a novel Nek-family kinase causes cystic kidney disease in the mouse and in zebrafish

**Shanming Liu[1], Weining Lu[1], Tomoko Obara[2], Shiei Kuida[1], Jennifer Lehoczky[3], Ken Dewar[3], Iain A. Drummond[2] and David R. Beier[1,*]**

[1]Genetics Division, Brigham and Women's Hospital, Harvard Medical School, Boston, MA, USA
[2]Renal Unit, Massachusetts General Hospital, Boston, MA, USA
[3]Whitehead Institute for Biomedical Research/MIT Center for Genome Research, Cambridge, MA, USA
*Author for correspondence (e-mail: beier@rascal.med.harvard.edu

*Accepted 23 September 2002*

## SUMMARY

**The murine autosomal recessive juvenile cystic kidney (*jck*) mutation results in polycystic kidney disease. We have identified in *jck* mice a mutation in *Nek8,* a novel and highly conserved member of the Nek kinase family. In vitro expression of mutated *Nek8* results in enlarged, multinucleated cells with an abnormal actin cytoskeleton. To confirm that a defect in the *Nek8* gene can cause cystic disease, we performed a cross-species analysis: injection of zebrafish embryos with a morpholino anti-sense oligonucleotide corresponding to the ortholog of *Nek8* resulted in the formation of pronephric cysts. These results demonstrate that comparative analysis of gene function in different model systems represents a powerful means to annotate gene function.**

Key words: PKD, mouse models, zebrafish, Nek kinase

## INTRODUCTION

The rapid progress in characterization of mammalian genome sequence will facilitate the use of mouse mutants for understanding gene function, and for investigating how perturbations of biological pathways can result in disease. Polycystic kidney disease (PKD) represents a major cause of human morbidity and mortality. Although *PKD1* and *PKD2*, the genes responsible for the great majority of human autosomal dominant PKD, have both been cloned, the biological basis of this disorder is not understood (American PKD1 Consortium, 1995; European Polycystic Kidney Disease Consortium, 1994; International PKD Consortium, 1995). Cystic degeneration in PKD is marked by the failure to maintain differentiated epithelial cell form and function; this is likely to involve multiple cell signaling pathways and cell structures, including those required for cell adhesion, maintainance of the cytoskeleton and epithelial cell polarity.

Genetic analysis of epithelial cyst formation in animal models will facilitate the molecular characterization of novel genes required for normal epithelial function and will contribute to understanding the cellular pathology of cystic disease. The juvenile cystic kidney (*jck*) mutation is a model of autosomal recessive PKD (Atala et al., 1993). The *jck* mutation was initially mapped to a 1.5 cM interval on mouse chromosome 11 (Iakoubova et al., 1995), and modifying loci affecting progression of PKD in this system have been identified (Iakoubova et al., 1999; Kuida and Beier, 2000). We describe the positional cloning of the gene mutated in *jck*, and the characterization of this defect using both in vitro analysis and a test of gene function in zebrafish embryos.

## MATERIALS AND METHODS

### Mice

C57BL/6J *jck*/+ mice are maintained in our mouse facility. FVB/N mice were obtained from Charles River Laboratories and *Mus castaneous* (CAST) mice were obtained from The Jackson Laboratory. For recombination analysis F1 B6/FVB *jck*/+ mice were intercrossed and affected progeny identified by palpation at 6-7 weeks of age. For analysis of the B6/CAST cross, all progeny were analyzed using the genetic markers *D11Mit116* and *D11Mit117*, and the single recombinant analyzed by progeny testing.

### Genomic analysis

BAC clones were screened from RPCI-23 Segment I mouse BAC library (BACPAC Resource, http://www.chori.org/bacpac/) using overlap oligos hybridization on high-density DNA filters (Ross et al., 1999). BAC DNA was isolated using anion-exchange columns (Qiagen) and BAC end sequence was obtained by ABI-377 sequencer (Applied Bioysytems). Overlap oligonucleotide probes were designed from BAC end sequence using online software Overgo Maker (http://genome.wustl.edu/gsc/overgo/overgo.html). For each BAC end sequence, a pair of oligonucleotides whose 3′ ends were complementary by eight bases was labeled with $^{32}$P dATP and $^{32}$P

dCTP by a Klenow fill-in reaction and used to probe the high-density DNA filters. One set of five high-density filters (22×22 cm) were prehybridized for 4 hours and hybridized for 16 hours at 60°C. The hybridization was performed in 50 ml hybridization solution which containing 1% BAS, 1 mM EDTA, 7% SDS and 0.5 M sodium phosphate. After hybridization, the filters were washed in 1.5×SSC, 0.1% SDS and 0.5×SSC, 0.1% SDS solution at 58°C for 1 hour. Positive clones were identified by autoradiogram. Sixteen STS markers were developed from published sequences, as well as end sequences of YAC clones and 129/Sv BAC clones we have previously localized to this region (data not shown). Hybridization with a pooled set of overlapping oligonucleotides identified 31 clones. These were then ordered based on their STS content, which was determined by hybridization using individual oligonucleotides. These clones covered the full length of the proximal region of the interval, with a minimal tiling path of 7 BACs (Fig. 1).

### Cloning

Kidney total RNA (3 μg) poly(A) RNA (1 μg) was reverse transcribed with Superscript II RNase $H^-$ – Reverse Transcriptase (Gibco/BRL) in 20 μl reaction mixture followed by a treatment of 1 μl RNase H (Gibco/BRL) at 37°C for 20 minutes. From this mixture, 1-2 μl was used as template for PCR using primers distributed across the presumptive *Nek8* transcript. The PCR products were resolved on an agarose gel, purified by QIAquick Gel Extract Kit (Qiagen), and sequenced. 5′ RACE and 3′ RACE were carried out using the Marathon cDNA Amplification Kit (Clontech) according to the manufacturer's instructions. Sequence analysis was carried out using Sequencher 3.1 software (Gene Codes) and the PFAM search server: http://pfam.wustl.edu/index.html. The GenBank Accession numbers of the sequences are AF407579 (mouse) and AF407580 (zebrafish). Analysis of the Multiple Choice Northern Blot (OriGene Technologies) was carried out by hybridization of an overgo-oligonucleotide derived from the 3′ domain of *Nek8* corresponding to the sequence 5′-GGGCAGCGTGCGCATGCGGAGGGCAGAGA-AGTCCCTGACC-3′.

### In vitro analysis

Wild-type and *jck Nek8* cDNAs were amplified using primers containing 5′ terminal *Eco*RI sites and cloned into the HA-epitope-containing vector PuHD-P2 (kindly provided by Dr Kun-Ping Lu). Fragments from plasmids containing cDNA cloned in-frame after the HA epitope tag were transferred to the pcDNA3 mammalian expression vector (Invitrogen). A kinase-defective HA-tagged *Nek8* clone carrying a Lys-to-Met mutation at amino acid 33 was generated using the strategy described by Cormack (Cormack, 1998). Cos7, MDCK and Swiss 3T3 cells were cultured as monolayers in Dulbecco's Modified Eagle's Medium (Gibco/BRL) supplemented with 10% fetal bovine serum and antibiotic. Cells were maintained in a humid incubator at 37°C in a 5% $CO_2$ enviroment. Cells were transfected using SuperFect Transfection Reagent (Qiagen) according to the manufacturer's protocol. For transient gene expression study, transfected cells were fixed for immunostaining after a further culture of 1-3 days; For the establishment of stable transfected cell lines, cells were passed at 1:10 or 1:15 into selective medium containing 400 μg/ml G418 1-2 days after transfection and single colonies were picked up and split into fresh selective medium. For immunohistochemistry cells were fixed with 3.7% formaldehyde in PBS for 10-30 minutes, washed with PBS for 5 minutes, and permealized and blocked in blocking buffer [2% normal goat serum (Sigma), 0.4% Triton X-100 (Sigma) in PBS] for 15 minutes at room temperature. Cells were incubated with an appropriate dilution of primary antibody in blocking buffer for 2 hours at room temperature or at 4°C overnight. Cells were washed three times with washing buffer (0.2% Triton X-100 and 0.2% BSA in PBS) for 20 minutes each time, incubated with a proper dilution of fluorochrome-conjugated secondary antibody and DAPI in PBS containing 0.1% Triton X-100 at room temperature for 1 hour, and then washed twice with washing buffer for 20 minutes each time. Coverslips with stained cells were mounted in Vectashield (Vector Laboratories) and sealed with nailpolish. Primary antibodies used for immunostaining cultured cells included mouse anti-HA monoclonal antibody clone 12CA5 (Boehringer Mannheim) (1:1,000 dilution of 0.4 mg/ml stock solution); mouse monoclonal anti-α-tublin FITC-conjugated antibody (Sigma) (1:50 dilution); and rabbit anti-γ-tubulin antibody (Sigma) (1:1000 dilution). Secondary antibodies included Cy3-conjugated goat anti-mouse IgG (Jackson ImmunoResearch Laboratories) (1:100 dilution of 0.7 mg/ml stock stock solution) and FITC-conjugated goat anti-rabbit IgG (Sigma) (1:80 dilution), Other histochemical reagents included 0.1 mg/ml FITC-labeled phalloidin (Sigma) used at 1:20 dilution and 1 mg/ml DAPI (Sigma) used at 1:1000 dilution. Images were aquired at the Brigham and Women's Confocal and Multiphoton Imaging facility, using a BioRad 1024 MP confocal system.

### Antibody synthesis and analysis

A DNA fragment carrying the *Nek8* C-terminal RCC domain (285-698 amino acids) was amplified using primer pair pET-*Bam*HI-F: CGGGATCCCGCCTATAGCCTCTGGCAGCAC and pET-*Eco*RI-R: CGGAATTCCCATTGACGACACAATCCAG and cloned into vector pET-30c after digestion with *Bam*HI and *Eco*RI. This was transformed it into BL21(DE3)PlysS competent cells. IL cultures were grown, induced with IPTG (1 mM), spun down and frozen overnight. BugBuster Protein Extraction Reagent (Novagen) was used to to purify inclusion bodies and the expressed protein purified using His-Bind Purification Kit (Novagen). Serum from rabbits immunized with purified protein was obtained from a commercial provider (ProSci). The antibody was affinity-purified using the His-tagged protein bound to an AminoLink Plus Coupling Gel (Pierce Biotechnology). Western analysis with affinity-purified antibody identifies a single 75 kDa band in cells transiently or stably transfected with a *Nek8* expression vector (data not shown). Two-week-old wild-type and mutant mice were sacrificed and tissues fixed by perfusion with 4% paraformaldehyde. Frozen sections (5 μm) were incubated briefly in 1% SDS/PBS to enhance antigenicity followed by washing and incubation for 1 hour at room temperature with affinity-purified Nek8 antibody (1:1000 dilution). As a secondary antibody, Cy3-conjugated Goat anti-Rabbit IgG (1:1000; Jackson immunochemicals) was used and microscopy was performed using a BioRad Radiance 2000 confocal microscope.

### Microscopy

Two-week-old juvenile kidneys were fixed overnight at 4°C in 2% glutaraldehyde/0.1 M sodium cacodylate (pH 7.2). For light microscopy, kidneys were embedded in glycol methacrylate, sectioned at 4 μm, stained using methylene blue/azure II (Humphrey and Pittman, 1974) and observed on a Nikon 800 microscope. For electron microscopy, kidneys were embeded in Epon using standard procedures (Majumdar and Drummond, 1999), sectioned and stained with uranyl acetate and lead citrate. Sections were observed and photographed using a Phillips CM10 electron microscope.

### Zebrafish analysis

Zebrafish *Nek8* was mapped on the T51 radiation hybrid map by the RH Mapping Service of The Children's Hospital Zebrafish Genome Initiative, under the direction of DrYi Zhou (http://zfrhmaps.tch.harvard.edu/ZonRHmapper/Default.htm#index). Two primer pairs were tested: Zfishnek1 (forward, CCCTGTTGGATGAGGACACT; reverse, GTGCTTGTCCAGGAGGATGT) and Zfishnek2 (forward, CAGCTCAGAATGAATGCCAA; reverse, TTGCGATCATTAGTG-CCTTG). Both were most tightly linked with the marker fj44a05.x1 on Linkage Group 15. Zebrafish embryos from wild-type pair matings (TL strain) were injected at the two-cell stage with a solution containing 0.2 mM *Nek8* antisense morpholino oligonucleotides (Gene-Tools LLC) in 200 mM KCl, and 0.1% Phenol Red. High doses of *Nek8* antisense oligos caused developmental arrest at the tail bud

stage, implying a role for *Nek8* in early development; five-fold less oligo injection allowed for bypassing early arrest and the analysis of organogenesis phenotypes. Final oligonucleotide concentration in the cytoplasm was estimated to be between 200 and 500 nM. The sequence of the translation blocking oligo was 5′-CTTCTCAT-ACTTCTCCATGTTTTCG-3′ (control); that of the randomized oligonucleotide (control) was 5′-CCTCTTACCTCAGTTACAATTT-ATA-3′; and that of the splice donor blocking oligonucleotide was 5′-CTAGGAGGCACACCTGTTAGGCAGG-3′ (splice junction at nt. 1281 of *Nek8*, GenBank AF407580). Injection of control oligo showed no effect on development. Control and experimental embryos were maintained at 28.5°C in egg water (46) and allowed to develop to 48-60 hours post fertilization (hpf). Embryos were fixed and processed for histology or for purification of total RNA. Nested RT-PCR primers in exons flanking the blocked splice donor site were used to confirm oligo efficacy and characterize the altered mRNA splicing product (final forward primer, 5′-CTACACCTGGGGCAGTGGCAT-TT-3′; final reverse primer, 5′-TGGCTATCCTGAGTGGCCAAACC-3′). Amplification of β-actin was performed as a control for semi-quatitative RT-PCR and showed equal amplification in all samples.

## RESULTS

To localize the mutation further, a genetic analysis of $F_2$ progeny of an intercross between C57BL/6J *jck* and FVB/N mice was carried out, which demonstrated that the *jck* mutation lies between the markers *D11Mit116* and *D11Mit117* (see Materials and Methods). In over 520 meioses, three recombinants between these markers were found, corresponding to a genetic distance of 0.58±0.33 cM. This interval includes the *nude* (*Whn/Foxn1*) locus, and four BACs covering 325 kb in this region have been fully sequenced (Fig. 1). However, analysis of this region indicates this is a physical interval of more than 1 Mb (Segre et al., 1995). Furthermore, these investigators identified a gap in the proximal end of this interval, which is also not covered in the contig described by Nehls et al. (Nehls et al., 1994). We therefore developed a sequence-ready BAC contig across the uncharacterized region (Fig. 1).

The utility of the recombinants previously identified between *D11Mit116* and *D11Mit117* was limited because of the lack of informative markers between inbred laboratory strains in this region. We therefore initiated a cross between C57BL/6J *jck* mice and *Mus castaneus*, and identified one recombinant between *D11Mit116* and *D11Mit117* in 283 $F_2$ progeny. Analysis of the recombinant using informative SSLPs from BAC end sequences narrowed the interval containing *jck*. Three BACs covering the *jck* interval and extending to the previously sequenced region were identified (Fig. 1) and sequenced.

BLAST homology searches identified several genes on these BACs, including one with homology to the Nek (NIMA-related) family of serine-threonine kinases. This was of note because a mutation in a different family member, *Nek1*, has been shown to cause a similar polycystic kidney phenotype in the *kat* mutant mouse (Upadhya et al., 2000). Nek family members 1-7 have been previously described; we have therefore named this novel family member *Nek8*. The full-length sequence of the mouse *Nek8* mRNA was determined using RT-PCR and 5′ and 3′ RACE. *Nek8* mRNA contains a 698 amino acid open reading frame that encodes both an N-terminal Nek kinase domain and C-terminal domains homologous to repeated motifs found in the regulator of chromatin condensation (RCC) gene (Fig. 2). Northern expression analysis of mouse *Nek8* demonstrated the expected approximately 3 kb transcript present most abundantly in kidney and liver, and a larger transcript present in testes (Fig. 2).

Sequence comparison of the *Nek8* transcripts in wild-type

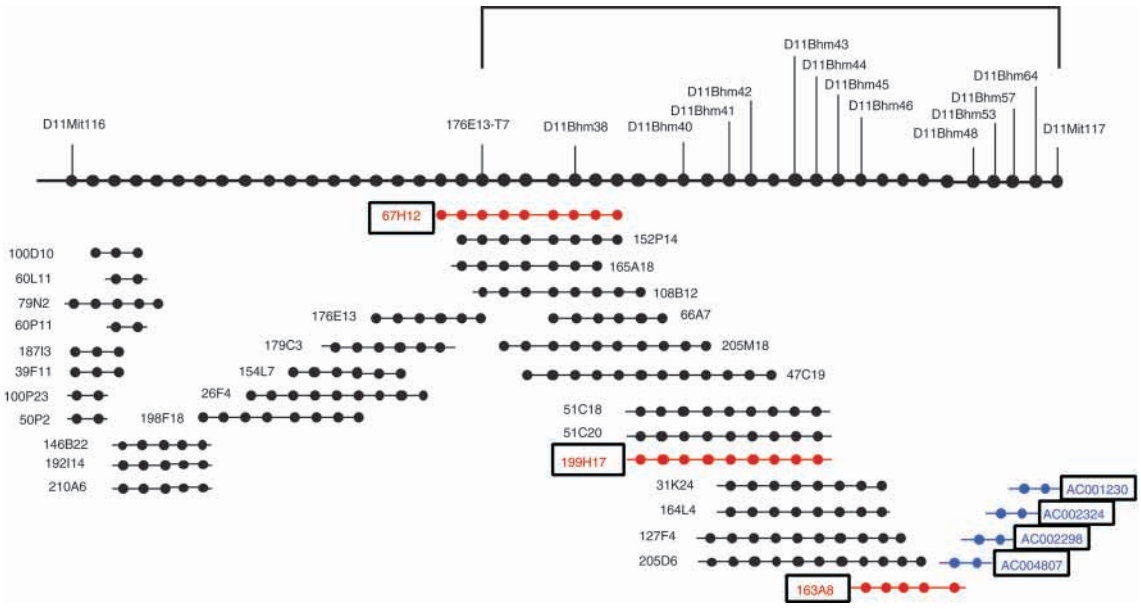


**Fig. 1.** Genetic and physical interval between *D11Mit116* and *D11Mit117* containing the *jck* mutation. The positions of STS markers, microsatellite markers and BAC clones are shown (not to scale). The brackets define the recombinant interval defined using a cross between B6 *jck* and *Mus castaneus* mice (see text). The boxed clones have been sequenced (67H12 is Accession Number AC025628; 199H17 is Accession Number AC022781; and 163A8 is Accession Number AC048361). *Nek8* is located on clone 163A8.

and *jck* mice revealed two sequence changes; both are mutations of guanine nucleotides to thymidine, at bp 1346 and 1348, respectively (Fig. 2). The former nucleotide change is silent, while the latter results in a non-conservative substitution of valine for glycine. This sequence variation is not present in wild-type C57BL/6J genomic DNA, which is the parental strain in which the spontaneous *jck* mutation occurred. The mutated glycine is strictly conserved in all other vertebrate *Nek8* homologs (Fig. 2).

An affinity-purified polyclonal antibody generated against a peptide derived from the C-terminal 413 amino acids of *Nek8* reveals that it is specifically located in the apical cytoplasm of collecting duct epithelial cells (Fig. 3). In *jck* mutant kidneys this localization is lost, even prior to the formation of overt kidney cysts (Fig. 3) and instead, *Nek8* is localized diffusely in the cytoplasm.

To assess the functional consequences of the amino acid substitution, we made epitope-tagged wild-type and *jck* mutant *Nek8* constructs for expression in cell culture (see Materials and Methods). We also generated a kinase-defective *Nek8* construct containing a substitution of methionine for lysine at amino acid 33, a mutation of the ATP binding loop that abrogates function of the homologous NIMA kinase (Lu and Means, 1994). Transient transfection of these constructs into Cos7, 3T3 and MDCK cells had dramatic consequences: although cells expressing wild-type *Nek8* appeared normal, cells expressing the *jck* mutant or kinase-defective *Nek8* became enlarged and multinucleated (Fig. 4). The effect of the *jck* mutant *Nek8* gene is equally severe as that of the kinase-mutant construct. In all cases the epitope-tagged *Nek8* protein appeared localized in the cytoplasm, although low levels of expression in the nucleus cannot be excluded. Expression of an appropriate size protein in the transfected populations was confirmed by western blot analysis (data not shown). Expression of the *jck* and kinase-defective mutant forms had similar but less severe effects in stably transfected cells, although the expression of the protein was significantly lower. Given its effect in transient expression assays, it is likely there is selection against cells that express high levels of abnormal *Nek8* protein.

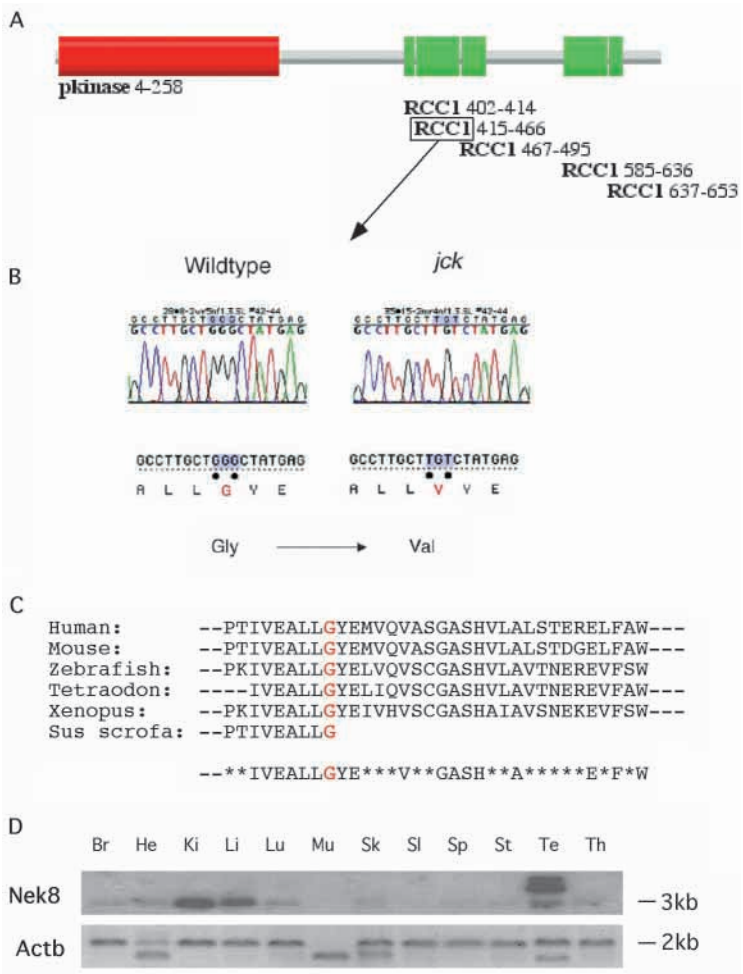


**Fig. 2.** The *Nek8* gene is mutated in *jck* mice. (A) Protein domain structure of the murine NEK8 protein (analysis carried out using the PFAM search server: http://pfam.wustl.edu/index.html). (B) Sequence changes at bp 1346 and 1348 in the *jck* mutant mouse result in a Gly-to-Val substitution at amino acid 448. (C) Conservation of the region containing the *jck* mutation across species. Mouse and zebrafish sequence determined as described in the text, human sequence is from multiple ESTs (Accession Numbers BF795289, BG755480 and AA076459), *Sus scrofa* sequence is from an EST (Accession Number BF189288), *Tetraodon* sequence is from a genomic survey sequence (Accession Number AL324795), *Xenopus* sequence is from an EST (Accession Number BE132147). (D) Northern analysis of *Nek8* and *Actb* (β actin) control. Br, brain; He, heart; Ki, kidney; Li, liver; Lu, lung; Mu, muscle; Sk, skin; Sl, small intestine; Sp, spleen; St, stomach; Te, testes; Th, thymus.

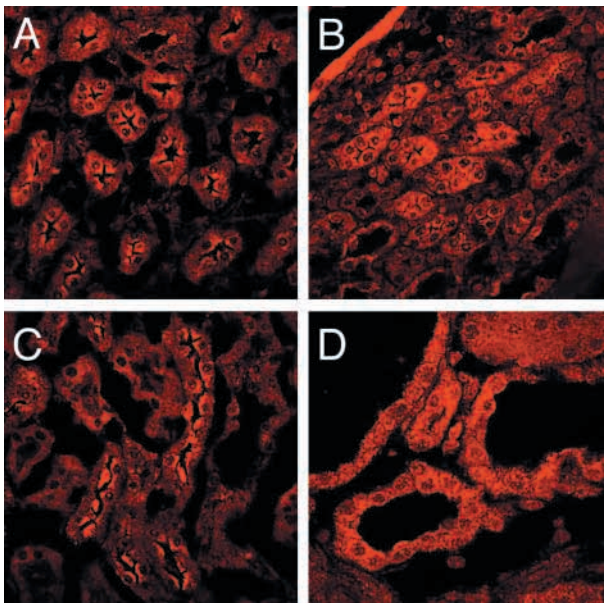


**Fig. 3.** Immunohistochemical localization of *Nek8*. Confocal immunofluorescence microscopy using affinity-purified anti-*Nek8* revealed strong expression in the apical cytoplasm of two-week-old wild-type inner medullary collecting duct cells (A) shown in cross-section. Similar sections from $jck^{-/-}$ kidneys (B) show diffuse cytoplasmic *Nek8* staining, often appearing as a perinuclear ring. Wild-type cortical collecting ducts also showed strong apical expression of *Nek8* (C), while cystic collecting duct epithelia in $jck^{-/-}$ tissue (D) show a diffuse pattern of cytoplasmic expression.

The enlarged and multinucleated appearance of cells expressing *jck* mutant and kinase-defective *Nek8* proteins is similar to that described for cells in which the actin or microtubule cytoskeletal networks have been disrupted (Andreassen and Margolis, 1994; Court and Moore, 1985). Immunohistochemical analysis of MDCK cells expressing *jck* mutant and kinase-defective *Nek8* showed no clear effect on microtubules (data not shown), but demonstrate a marked reduction of actin stress fibers (Fig. 4).

Histological analysis of *jck* mutant kidney tubules showed no nuclear abnormalities, and immunohistochemical studies using antibodies against specifically apical or basolateral membrane proteins (aquaporin2, H+ ATPase, anion exchanger AE1/2, Na+K+ ATPase and tubulin) showed no evidence of membrane protein mislocalization (data not shown). However, light and electron microscopy revealed a consistent defect in the tubular epithelia of mutant kidneys; specifically, the integrity and structure of basal membrane infoldings (i.e. the basal labyrinth) were disrupted and epithelial cells were in some cases observed to detach from the basement membrane (Fig. 5). These defects were specific to the connecting segment and collecting duct cells; proximal tubule cells appeared morphologically normal (data not shown). Cell membrane and cytoplasmic disruption could be observed in connecting segments and collecting ducts with normal lumen diameters from mutant mice 2-3 weeks of age, indicating that the cellular defects preceded overt cyst formation. Cell-cell junctions in *jck* cysts looked morphologically normal when examined by electron microscopy, indicating that the cyst phenotype is not primarily a consequence of disruption of adherens junction formation (data not shown).

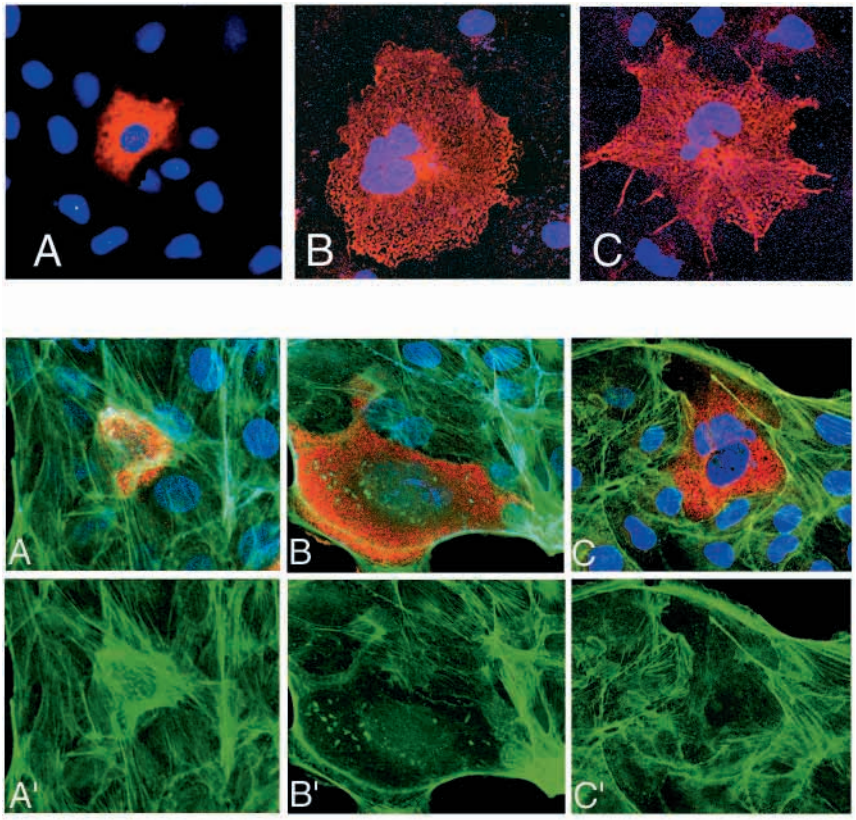


**Fig. 4.** Effect of transient expression of wild-type and mutant Nek8 in cultured cells. (Top) Images of Cos7 cells stained with anti-HA monoclonal antibody and DAPI after transfection with (A) wild-type, (B) *jck* or (C) kinase-deficient *Nek8*. Transfection with the mutant *Nek8* kinases results in enlarged, multinucleated cells. (Bottom) Images of MDCK cells stained with anti-HA monoclonal antibody, phalloidin and DAPI after transfection with (A) wild-type, (B) *jck* or (C) kinase-deficient *Nek8*. Staining with phalloidin alone is shown in A′, B′ and C′. The *Nek8* protein is expressed predominantly in the cytoplasm, and actin stress fibers are reduced in cells that express the mutant *Nek8* kinases.

To confirm that a defect in *Nek8* can result in cystic disease we took advantage of the observation that morpholino antisense oligonucleotides (MO) can be used to abrogate gene function in zebrafish, resulting in several cases in phenotypes indistinguishable from proven null mutations (Nasevicius and Ekker, 2000). We identified an EST from zebrafish with significant homology to *Nek8* (Accession Number, BG302641) and determined its full-length sequence, which showed 72% amino acid identity and 84% similarity to murine *Nek8*, and also carried both the Nek and RCC domains in a single open reading frame. Analysis of the T51 radiation hybrid panel (Geisler et al., 1999) localized zebrafish *nek8* to chromosome 15, which has conserved synteny with mouse chromosome 11 and human chromosome 17 (Woods et al., 2000), further supporting this gene as the zebrafish ortholog of *Nek8*. Specifically, zebrafish *nek8* is tightly linked with the marker fj56h04.x1, which is derived from an EST that has strong homology to the mouse gene *Aldo3*, which maps within the recombinant interval containing *jck* (Segre et al., 1995).

Morpholino antisense oligonucleotides were designed to interfere with *Nek8* translation (by binding to the initiation ATG codon) or mRNA splicing (by blocking splice donor sites). Microinjection of both translation blocking and splice donor blocking antisense oligos into two-cell stage embryos resulted in the development of severe pronephric cysts as early as 48 hours post fertilization (Fig. 6). This stage of development corresponds to the onset of kidney function at hatching (Drummond et al., 1998). The timing and morphology of pronephric cyst formation in *Nek8* MO-injected embryos closely resembles cyst formation in a previously characterized group of pronephric kidney mutants (Drummond et al., 1998). In some cases, pronephric duct cells could be observed detached from the basement membrane and present in pronephric duct lumens (data not shown), a phenotype similar to the cysts seen in the *jck* mouse collecting ducts.

## DISCUSSION

Using a positional cloning strategy we have identified a novel member of the Nek kinase family and found it is mutated in the *jck* mouse. A number of observations support the

conclusion that the sequence changes found in the C-terminal domain of *Nek8* can cause PKD. First, the sequence change is in *jck* mutants, but not in the parental C57BL/6J strain in which the mutation occurred. Second, the sequence change is a non-conservative amino acid substitution in a highly conserved amino acid motif, present in species evolutionarily distant from mammals including *Xenopus* and *Tetraodon*. Additionally, in vitro analysis demonstrates that this substitution has dramatic functional consequences, equally severe as that of a *Nek8* gene carrying a null mutation in its kinase domain. Last, interference of zebrafish *Nek8* mRNA translation using morpholino antisense oligonucleotides results in the development of pronephric cysts, demonstrating in a different species that *Nek8* is required for renal tubular integrity.

The Nek protein kinase family is defined by their similarity to the NIMA (never in mitosis A) kinase found in *Aspergillis nidulans*. Although overexpression of mutant NIMA kinase in mammalian cells also disrupts the cell cycle (Lu and Hunter, 1995), none of the mammalian Nek genes has been shown to have a similar effect, suggesting that the function of the Nek family of kinases is broadly diversified. A striking aspect of the Nek family is that, while their kinase domains show significant amino acid similarity, many (but not all) of these family members have distinctive, presumptive regulatory, C-terminal domains. The C-terminal domain of *Nek8* has multiple repeats of a protein motif found in RCC1, a protein that is required for normal chromosome condensation in yeast. *Drosophila* appears to have only two Nek family protein kinases. One is CG10951 (33% identity and 48% similarity), which contains both the Nek and RCC domains. The second, CG17256, has an N-terminal Nek domain but has a C-terminal region that is not conserved in mammals. Recently, a human Nek family member with a high degree of homology to *Nek8* has been characterized (Holland et al., 2002). This protein, which localizes to human chromosome 14q24 (AC007055; BAC clone 201F1), is not the ortholog of mouse *Nek8*; the true ortholog is in the appropriate region of conserved synteny on chromosome 17q11 (AC010761; BAC clone RP11-386F9). Analysis of this Nek-family kinase, which has been assigned the name *Nek9*, in transient expression assays suggests that it interacts with *BICD2*, the mammalian homolog of Drosophila *Bicaudal D*. Mutations in *Bicaudal D* affect the organization and polarization of the microtubule network during oogenesis (Mach and Lehmann, 1997; Theurkauf et al., 1993) and BICD2 co-localizes with microtubule-associated proteins (Hoogenraad et al., 2001). *Nek9* has also been found to bind the *Ran* GTPase when co-expressed in cultured cells (Roig et al., 2002). Whether this interaction occurs in vivo has not yet been addressed.

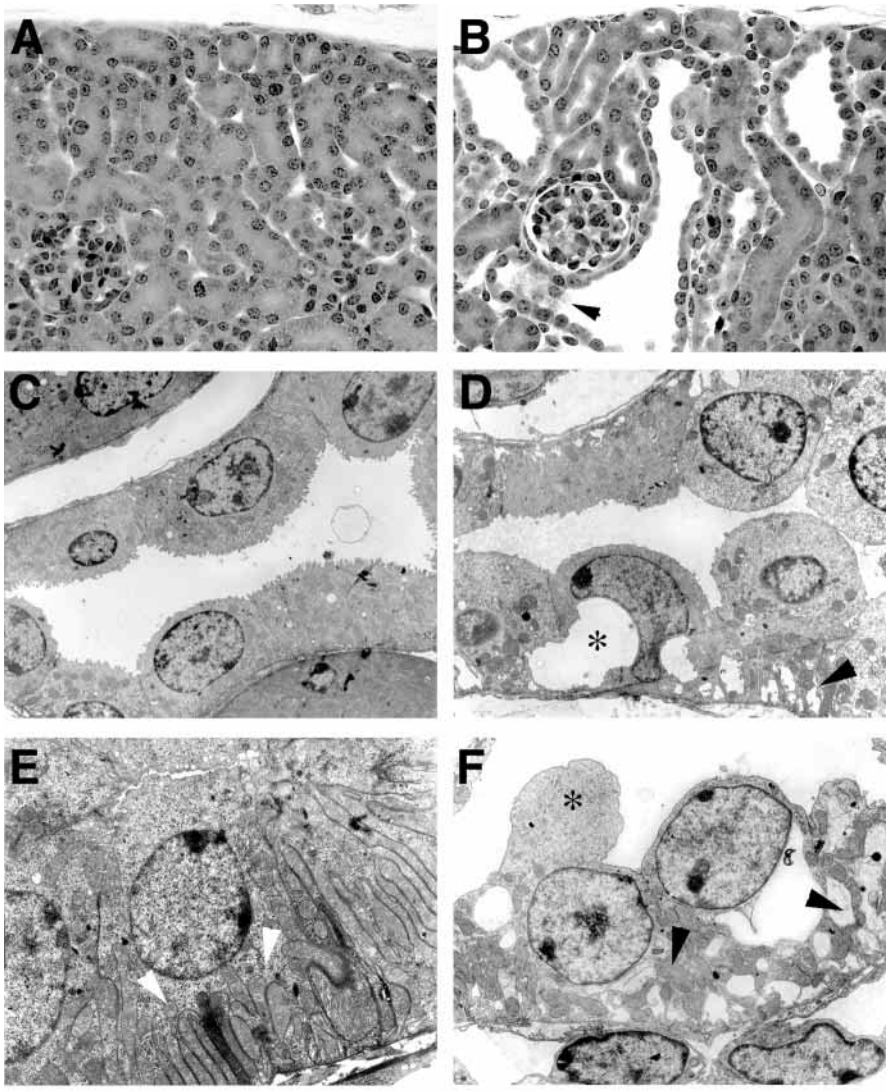


**Fig. 5.** Epithelial cell adhesion and cytoplasmic organization are disrupted in *jck*$^{-/-}$ kidneys. Light micrographs of kidney sections from two-week-old wild-type (A) and *jck*$^{-/-}$ (B) mice from the kidney cortex. Tissue from *jck* mutants shows cyst formation in the connecting segments and cortical collecting ducts with evidence of cell detachment in the cyst lumens (arrowhead in B). Proximal tubules and glomeruli are not grossly affected in *jck* kidneys. Electron micrographs of wild type (C) and *jck* collecting ducts (D) reveal distension of the basal labyrinth in *jck* epithelia with large vacuolations (asterisk in D) and early signs of cell heightening and detachment (arrowhead in D) prior to overt cyst formation. Basal infoldings seen surrounding mitochondria in wild-type connecting segment cells (white arrowheads in E) are severely disrupted in *jck* connecting segments (arrowheads in F) and cellular organization is lost with large protrusions of cytoplasm extending into the forming cyst lumen (asterisk in F).

Our results suggest that an essential function of *Nek8* may be to regulate local cytoskeletal structure in kidney tubule epithelial cells. Wild-type *Nek8* is localized specifically to the apical cytoplasm of collecting duct epithelial cells. When mutated, *Nek8* is mislocalized diffusely in the cytoplasm, often appearing in a perinuclear ring, while cytoskeletal organization is grossly disorganized and

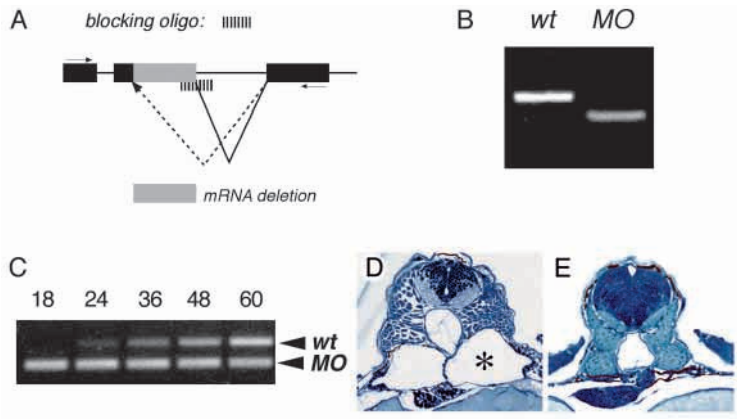


**Fig. 6.** Pronephric cyst formation in Nek8 antisense oligonucleotide injected zebrafish embryos. (A) Splice donor blocking oligo (see Materials and Methods) disruption of *Nek8* mRNA splicing. Sequence analysis of the resulting aberrant *Nek8* mRNA in 24 hpf embryos by RT-PCR (B) showed that this oligo induced a 129 nucleotides (43 amino acid) in-frame deletion corresponding to the first RCC1 homology domain C-terminal to the Nek kinase domain. (C) Time course quantification of oligo efficacy showed complete absence of wild-type mRNA at 18 hpf and a gradual recovery of wild-type message by 24-60 hpf. (D) Histological analysis of embryos injected as in C show severe pronephric cysts (*) at 60 hpf. (E) Injection of control random oligo (500 nM cytoplasmic concentration) or lower doses of the splice donor blocking oligo (50 nM cytoplasmic concentration) produces normal pronephric kidney formation at 60 hpf.

apical cytoplasmic protrusions are observed. Overexpression of mutated *Nek8* in cultured cells results in multinucleation, cell enlargement and a loss of actin stress fibers, further suggesting a failure to properly regulate the actin cytoskeleton. Tubule cells in *jck* mutant mice are not multinucleated; however, given the importance of the cytoskeleton in cellular functions such as the maintenance of polarity and cell adhesion, we speculate that a more subtle defect of cytoskeletal regulation in these cells results in cyst formation. Significantly, the kidney epithelial phenotype of the *jck* mouse closely resembles the phenotype of a Rho GDIα knockout mouse. The mutation in Rho GDIα results in disruption of the basal cytoplasmic organization in connecting segment/collecting duct epithelial cells and cystic dilation (Togawa et al., 1999). The Rho family of small GTPases has been shown to play a central role in actin cytoskeletal regulation in general and in stress fiber assembly specifically (Kaibuchi et al., 1999). Rho is also known to have a role in the regulation of cytokinesis; for example, expression of a dominant-negative Rho-kinase mutant in *Xenopus* embryos and mammalian cells inhibits this process and results in multinucleated cells (Yasui et al., 1998).

Our observation that the *jck* mutation is in a kinase that may be required for normal cytoskeletal function is of note in the context of a growing body of evidence implicating defects in components of the cell-matrix and cell-cell adhesion systems as a fundamental cause of cystic kidney disease (Wilson, 2001). Most notably, the *Pkd1* gene, which is the locus mutated in the most common form of human PKD, encodes polycystin, a large transmembrane protein with multiple extracellular domains implicated in cell-cell adhesion. Polycystin has been localized to multiple sites involved in adhesion including adherens junctions, desmosomes and focal adhesion complexes (Geng et al., 2000; Huan and van Adelsberg, 1999; Scheffers et al., 2000). Defects in other protein components of the focal adhesion complex can result in cystic disease; specifically, α-actinin (in human focal glomerulosclerosis) (Kaplan et al., 2000), nephrocystin (in medullary cystic disease) (Hildebrandt et al., 1997) and tensin (in targeted mutations in the mouse) (Lo et al., 1997).

Because we only have a single allele of *jck*, we chose to confirm that *Nek8* was the causal defect using a cross-species analysis in zebrafish, and we recommend this as a general strategy for assessing gene function. This is especially important given the resurgence of interest in using ENU mutagenesis for generating novel murine models of disease and development. While ENU mutagenesis is extremely efficient, the logistics of this analysis in mice generally precludes reaching saturation, and it is likely that many of the mutations identified by these screens will be single alleles. Furthermore, treatment with ENU usually generates single nucleotide changes, and, in the cases where they have been characterized, nearly two-thirds of these were found to be missense changes (Noveroske et al., 2000), the functional consequences of which may not necessarily be easily tested. Analysis of candidate gene function in zebrafish represents an attractive strategy because it is inexpensive, technically straightforward, and most importantly, rapid; especially compared with murine transgenesis techniques, which would require a minimum of two generations to confirm a functional defect. We suggest that the combined forward and reverse genetic approaches using the mouse and zebrafish can be a highly efficient method of determining gene function.

This work was funded by DK4563902 (D. R. B.), DK53093 (I. A. D.), DK54711 (D. R. B. and I. A. D.), and with the generous support of the PKR Foundation. We thank O. Iakoubova, J. Segre, I. Neuhaus, K. P. Lu, Y. Zhou and the members of the WI/MIT Center for Genome Research Sequencing Group for their contributions to this work.

## REFERENCES

**American PKD1 Consortium** (1995). Analysis of the genomic sequence for the autosomal dominant polycystic kidney disease (PKD1) gene predicts the presence of a leucine-rich repeat. The American PKD1 Consortium (APKD1 Consortium). *Hum. Mol. Genet.* **4**, 575-582.

**Andreassen, P. R. and Margolis, R. L.** (1994). Microtubule dependency of p34cdc2 inactivation and mitotic exit in mammalian cells. *J. Cell Biol.* **127**, 789-802.

**Atala, A., Freeman, M. R., Mandell, J. and Beier, D. R.** (1993). Juvenile cystic kidneys (jck): a new mouse mutation which causes polycystic kidneys. *Kidney Intl.* **43**, 1081-1085.

**Cormack, B.** (1998). Current protocols in molecular biology. In *Current Protocols in Molecular Biology*, Vol. 1 (ed. F. Ausubel, R. Brent, R. Kingston, D. Moore, J. Seidman, J. Smith and K. Struhl). New York: John Wiley and Sons.

**Court, J. B. and Moore, J. L.** (1985). The survival of cytochalasin-induced multinucleation following irradiation of Chinese hamster ovary cells. *Cell Biol. Int. Rep.* **9**, 219-227.

**Drummond, I. A., Majumdar, A., Hentschel, H., Elger, M., Solnica-Krezel, L., Schier, A. F., Neuhauss, S. C., Stemple, D. L., Zwartkruis, F., Rangini, Z. et al.** (1998). Early development of the zebrafish pronephros and analysis of mutations affecting pronephric function. *Development* **125**, 4655-4667.

**European Polycystic Kidney Disease Consortium** (1994). The polycystic

kidney disease 1 gene encodes a 14 kb transcript and lies within a duplicated region on chromosome 16. *Cell* **77**, 881-894.

**Geisler, R., Rauch, G. J., Baier, H., van Bebber, F., Brobeta, L., Dekens, M. P., Finger, K., Fricke, C., Gates, M. A., Geiger, H. et al. (**1999). A radiation hybrid map of the zebrafish genome. *Nat. Genet.* **23**, 86-89.

**Geng, L., Burrow, C. R., Li, H. P. and Wilson, P. D.** (2000). Modification of the composition of polycystin-1 multiprotein complexes by calcium and tyrosine phosphorylation. *Biochim. Biophys. Acta* **1535**, 21-35.

**Hildebrandt, F., Otto, E., Rensing, C., Nothwang, H. G., Vollmer, M., Adolphs, J., Hanusch, H. and Brandis, M.** (1997). A novel gene encoding an SH3 domain protein is mutated in nephronophthisis type 1. *Nat. Genet.* **17**, 149-153.

**Holland, P. M., Milne, A., Garka, K., Johnson, R. S., Willis, C. R., Sims, J. E., Rauch, C. T., Bird, T. A. and Virca, G. D.** (2002). Purification, cloning and characterization of Nek8, a novel NIMA-related kinase, and its candidate substrate Bicd2. *J. Biol. Chem.* **25**, 25.

**Hoogenraad, C. C., Akhmanova, A., Howell, S. A., Dortland, B. R., de Zeeuw, C. I., Willemsen, R., Visser, P., Grosveld, F. and Galjart, N.** (2001). Mammalian Golgi-associated Bicaudal-D2 functions in the dynein-dynactin pathway by interacting with these complexes. *EMBO J.* **20**, 4041-4054.

**Huan, Y. and van Adelsberg, J.** (1999). Polycystin-1, the PKD1 gene product, is in a complex containing E-cadherin and the catenins. *J. Clin. Invest.* **104**, 1459-1468.

**Humphrey, C. and Pittman, F.** (1974). A simple methylene blue-azure II-basic fuchsin stain for epoxy-embedded tissue sections. *Stain Technol.* **49**, 9-14.

**Iakoubova, O., Dushkin, H. and Beier, D.** (1995). Localization of a murine recessive polycystic kidney disease mutation and modifying loci which affect disease severity. *Genomics* **26**, 107-114.

**Iakoubova, O., Dushkin, H., Pacella, L. and Beier, D. R.** (1999). Genetic analysis of modifying loci on mouse chromosome 1 that affect disease severity in a model of recessive PKD. *Physiol. Genomics* **1**, 101-105.

**International PKD Consortium** (1995). Polycystic kidney disease: the complete structure of the PKD1 gene and its protein. *Cell* **81**, 289-298.

**Kaibuchi, K., Kuroda, S. and Amano, M.** (1999). Regulation of the cytoskeleton and cell adhesion by the Rho family GTPases in mammalian cells. *Annu. Rev. Biochem.* **68**, 459-486.

**Kaplan, J. M., Kim, S. H., North, K. N., Rennke, H., Correia, L. A., Tong, H. Q., Mathis, B. J., Rodriguez-Perez, J. C., Allen, P. G., Beggs, A. H. et al.** (2000). Mutations in ACTN4, encoding alpha-actinin-4, cause familial focal segmental glomerulosclerosis. *Nat. Genet.* **24**, 251-256.

**Kuida, S. and Beier, D. R.** (2000). Genetic localization of interacting modifiers affecting severity in a murine model of polycystic kidney disease. *Genome Res.* **10**, 49-54.

**Lo, S. H., Yu, Q. C., Degenstein, L., Chen, L. B. and Fuchs, E.** (1997). Progressive kidney degeneration in mice lacking tensin. *J. Cell Biol.* **136**, 1349-1361.

**Lu, K. P. and Hunter, T.** (1995). Evidence for a NIMA-like mitotic pathway in vertebrate cells. *Cell* **81**, 413-424.

**Lu, K. P. and Means, A. R.** (1994). Expression of the noncatalytic domain of the NIMA kinase causes a G2 arrest in Aspergillus nidulans. *EMBO J.* **13**, 2103-2113.

**Mach, J. M. and Lehmann, R.** (1997). An Egalitarian-BicaudalD complex is essential for oocyte specification and axis determination in Drosophila. *Genes Dev.* **11**, 423-435.

**Majumdar, A. and Drummond, I. A.** (1999). Podocyte differentiation in the absence of endothelial cells as revealed in the zebrafish avascular mutant, cloche. *Dev. Genet.* **24**, 220-229.

**Nasevicius, A. and Ekker, S. C.** (2000). Effective targeted gene 'knockdown' in zebrafish. *Nat. Genet.* **26**, 216-220.

**Nehls, M., Pfeifer, D., Schorpp, M., Hedrich, H. and Boehm, T.** (1994). New member of the winged-helix protein family disrupted in mouse and rat nude mutations. *Nature* **372**, 103-107.

**Noveroske, J. K., Weber, J. S. and Justice, M. J.** (2000). The mutagenic action of N-ethyl-N-nitrosourea in the mouse. *Mamm. Genome* **11**, 478-483.

**Roig, J., Mikhailov, A., Belham, C. and Avruch, J.** (2002). Nercc1, a mammalian NIMA-family kinase, binds the Ran GTPase and regulates mitotic progression. *Genes Dev.* **16**, 1640-1658.

**Ross, M., LaBrie, S., McPherson, J. and Stanton, V.** (1999). Screening large-insert libraries by hybridization. In *Current Protocols in Human Genetics* (ed. N. C. Dracopoli, J. L. Haines, B. R. Korf, D. T. Moir, C. C. Morton, C. E. Seidman, J. G. Seidman and D. R. Smith), pp. 5.6.1-5.6.52. New York, NY: John Wiley and Sons.

**Scheffers, M. S., van der Bent, P., Prins, F., Spruit, L., Breuning, M. H., Litvinov, S. V., de Heer, E. and Peters, D. J.** (2000). Polycystin-1, the product of the polycystic kidney disease 1 gene, co- localizes with desmosomes in MDCK cells. *Hum. Mol. Genet.* **9**, 2743-2750.

**Segre, J. A., Nemhauser, J. L., Taylor, B. A., Nadeau, J. H. and Lander, E. S.** (1995). Positional cloning of the nude locus: genetic, physical, and transcription maps of the region and mutations in the mouse and rat. *Genomics* **28**, 549-559.

**Theurkauf, W. E., Alberts, B. M., Jan, Y. N. and Jongens, T. A.** (1993). A central role for microtubules in the differentiation of Drosophila oocytes. *Development* **118**, 1169-1180.

**Togawa, A., Miyoshi, J., Ishizaki, H., Tanaka, M., Takakura, A., Nishioka, H., Yoshida, H., Doi, T., Mizoguchi, A., Matsuura, N. et al. (**1999). Progressive impairment of kidneys and reproductive organs in mice lacking Rho GDIalpha. *Oncogene* **18**, 5373-5380.

**Upadhya, P., Birkenmeier, E. H., Birkenmeier, C. S. and Barker, J. E.** (2000). Mutations in a NIMA-related kinase gene, Nek1, cause pleiotropic effects including a progressive polycystic kidney disease in mice. *Proc. Natl. Acad. Sci. USA* **97**, 217-221.

**Wilson, P. D.** (2001). Polycystin: new aspects of structure, function, and regulation. *J. Am. Soc. Nephrol.* **12**, 834-845.

**Woods, I. G., Kelly, P. D., Chu, F., Ngo-Hazelett, P., Yan, Y. L., Huang, H., Postlethwait, J. H. and Talbot, W. S.** (2000). A comparative map of the zebrafish genome. *Genome Res.* **10**, 1903-1914.

**Yasui, Y., Amano, M., Nagata, K., Inagaki, N., Nakamura, H., Saya, H., Kaibuchi, K. and Inagaki, M.** (1998). Roles of Rho-associated kinase in cytokinesis; mutations in Rho-associated kinase phosphorylation sites impair cytokinetic segregation of glial filaments. *J. Cell Biol.* **143**, 1249-1258.